

Prediction of a Propellant Tank Pressure History Using State Space Methods

Paul N. Estey,* David H. Lewis Jr.,† and Maureen Connor‡

Jet Propulsion Laboratory, California Institute of Technology, Pasadena, California

An analysis of the time response of a propellant supply system operating in the blowdown mode is presented. The supply system is part of a pump-fed propulsion system intended for use on interplanetary spacecraft. As such, the supply system must provide the pump with propellant at sufficient pressure to avoid pump cavitation. The system, consisting of the tank, the liquid propellant, the pressurant gas and propellant vapor mixture, and a film layer separating the liquid and vapor phases, is analyzed using the principles of mass and energy conservation. The resulting set of ordinary, coupled, nonlinear differential equations for the thermodynamic state variables is integrated as an initial value problem. The resulting histories of total pressure, propellant vapor pressure, propellant liquid temperature, film layer temperature, propellant vapor/pressurant gas temperature, propellant vapor mass, and propellant liquid mass enable the calculation of the net positive suction head available at the pump which determines the viability of the pump-fed system concept when operated in the blowdown mode.

Nomenclature

a	= specified constant
A_g, A_f, A_t, A_w	= heat-transfer area
c_v, c_g	= specific heat at constant volume
c_t, c_w	= specific heat
D	= tank diameter
d	= liquid surface diameter
g	= gravity
Gr	= Grashof number
h_t, h_v	= enthalpy
h_{ts}, h_{vs}	= enthalpy at saturation
h_{fg}	= enthalpy of vaporization
h_g, h_f, h_s, h_t, h_w	= heat-transfer coefficient
k_ℓ	= thermal conductivity of the liquid
m_v, m_g, m_t, m_w	= mass
NPSH	= net positive suction head
n	= specified constant
p_{PI}, p_v, p_t, p_g	= pressure
R_v	= specific gas constant
$\dot{Q}_g, \dot{Q}_v, \dot{Q}_t, \dot{Q}_p, \dot{Q}_w$	= heat-transfer rate
T_v, T_t, T_f, T_w, T_a	= temperature
t	= time
Δt	= time step
u_1, \dots, u_r	= inputs
u_v, u_g, u_t, u_w	= internal energy
v	= specific volume of liquid propellant
V_t, V_v, V_g	= total volume
V_e, V	= velocity
\dot{W}	= work-transfer rate
y_i	= state variable
ρ	= density of liquid propellant
μ	= viscosity

Subscripts

a	= ambient
e	= engine

d	= based on liquid surface diameter
f	= film layer
g	= pressure gas
i	= inlet
ℓ	= propellant liquid
PI	= pump inlet
0	= initial value
s	= wetted tank surface
t	= tank or total
v	= propellant vapor
w	= tank wall

Superscripts

$()^*$	= dimensionless variable
$()'$	= derivative with respect to time (d/dt)
$()'$	= derivative with respect to dimensionless time (d/dt^*)

Introduction

IN the past it has been standard practice to use pressure-fed bipropellant propulsion systems to insert spacecraft into orbit about distant planets or the moon. These systems, such as the Viking orbiter, used the hypergolic propellant combination of nitrogen tetroxide (N_2O_4) and monomethylhydrazine (MMH). Studies have shown that for large orbit insertion velocity changes or large payload masses (corresponding to the propellant loads greater than 1000 lbm), a pump-fed orbit insertion propulsion unit (IPU) would save propulsion system dry mass over an equivalent pressure-fed system using N_2O_4 and MMH.¹⁻³ The pump-fed IPU utilizes two centrifugal pumps to supply the rocket engine with the proper mixture ratio and inlet pressure (see Fig. 1). In order to further decrease system dry mass, it is desirable to eliminate the propellant tank pressurization system entirely. If this is done, the propellant storage tanks operate in a blowdown mode and must supply the propellant to the pump inlet at a pressure sufficient to provide the minimum net positive suction head (NPSH) required by the pump. The NPSH available at the pump inlet is calculated from

$$NPSH = \frac{p_{PI} - p_v}{\rho} \quad (1)$$

where p_{PI} is the pressure at the pump inlet, p_v the vapor pressure of the propellant, and ρ the density of the liquid

Received Jan. 21, 1982; revision received Aug. 16, 1982. Copyright © 1982 by the American Institute of Aeronautics and Astronautics. All rights reserved.

* (Currently with Department of Mechanical Engineering, Stanford University, Palo Alto, Calif.).

† (Currently with TRW Space and Systems Group, Redondo Beach, Calif.).

‡ Jet Propulsion Laboratory.

propellant. Thus the local fluid pressure directly affects the NPSH. However, the fluid temperature also influences the NPSH calculation since liquid vapor pressure is a function of the liquid temperature. For purposes of this calculation the liquid density can be considered independent of temperature.

To determine the tank pressure history throughout an orbital insertion burn and thus determine if the NPSH delivered is sufficient for a given pump, a thermodynamic model of the tank and its contents was developed. This paper describes the development of the model and the results of a numerical solution of the thermodynamic equations for a typical orbital insertion-maneuver.

Although the motivation for development of the model was to analyze the pressure and temperature history of the tank in order to calculate the NPSH for the centrifugal pump, the analysis presented herein can be generalized to any supply system operating in a blowdown mode. This type of analysis is of greatest benefit when the liquid being stored has a sufficiently high vapor pressure such that it is a significant percentage of the total pressure in the tank.

Several models have been developed to predict tank pressure histories.⁴⁻¹² However, these models have been involved with either self-pressurization from a cryogenic propellant such as liquid hydrogen⁴⁻⁷ or model a pressurized tank with pressurant gas supplied from a separate high pressure storage tank.⁸⁻¹⁰ Reference 10 describes an entire pressure-fed system model that provides data on available impulse as a function of expulsion rate. This system incorporates a separate high-pressure pressurant storage tank, whereas Refs. 11 and 12 are concerned with propellant tanks operated in a blowdown mode. However, in both of these cases the flow rates are lower and the pressures higher than those considered here. The approach used in Ref. 11 is similar to that presented in this analysis; however, mass transfer from the liquid to gaseous state due to evaporation was assumed negligible. For the case of high operating pressure, roughly 300 psia (2.07 MPa) initially to 100 psia (0.689 MPa) at the end of blowdown, this is a good assumption as the propellant vapor pressure is a small percentage of the total pressure. However in the case of a blowdown at a lower initial pressure, ranging from approximately 70 to 17 psia (0.48-0.12 MPa), the propellant vapor pressure is a significant percent of the total tank pressure. Reference 12 describes the results of modeling a bipropellant blowdown propulsion system used for attitude control and stationkeeping over a long mission life, but it does not describe the model development or implementation.

In most of these previous studies finite-difference methods of numerical calculation were used to solve for the state variables (pressure, temperature, etc.) as functions of time. In the finite-difference method, the derivatives of state variables

are expressed as Taylor series expansions normally with the terms greater than first order truncated.

Generally one uses a forward-difference, hence explicit, scheme to approximate the derivatives of the state variables at time t , and thus the equations of conservation of energy and mass are solved to determine the new values of the state variables at time $t + \Delta t$. Since the method is explicit, instability will occur for large values of the time step Δt . An unconditionally stable implicit scheme can also be used to determine the derivatives; however, this requires iteration and increases computer run time. It is not expected that the system of equations is stiff as there are no disparities in any length or time scales; thus the conditionally stable explicit schemes are satisfactorily stable. Accuracy is dependent on the time step Δt taken. Smaller time steps yield more accurate solutions but also increase computer run time.

In this paper a distinctly different numerical technique is presented, the state space method. In the state space method of analysis the derivative of the i th state variable is expressed in terms of the local values of the state vector as well as the independent variable t and any inputs (forcing functions) $u_1 \dots u_r$. Thus implicit functional relationships such as

$$\frac{dy_i}{dt} = f(y_1 \dots y_n, t, u_1 \dots u_r) \quad (2)$$

are developed for each state variable. This set of first-order, ordinary, nonlinear differential equations (ODE) is then integrated numerically as an initial value problem using an iterative multistep predictor-corrector differencing technique. In this manner all of the system differential equations are solved simultaneously at every time step.

The advantages of this method are several. Stability is virtually assured, and accuracy is greater than first order. This method is accurate to at least second order, and fourth-order accuracy is possible. In the integration routine used, the time step is adjusted to meet a specified accuracy. When the derivatives are small, the time steps are increased and thus computer run time decreased.

Thermodynamic Model

A sketch of a propellant tank and contents is shown in Fig. 2. During the blowdown process, liquid is removed at a constant rate by the pump and consequently the gas mixture does work on the liquid as the mixture volume increases. Furthermore, there is mass transfer from the liquid to the gas mixture as the pressure decreases in the tank. In addition there is an exchange of mass and energy through the boundaries of

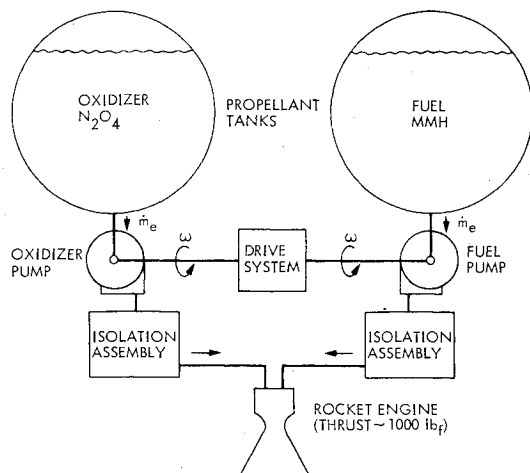


Fig. 1 Pump-fed propulsion system schematic drawing.

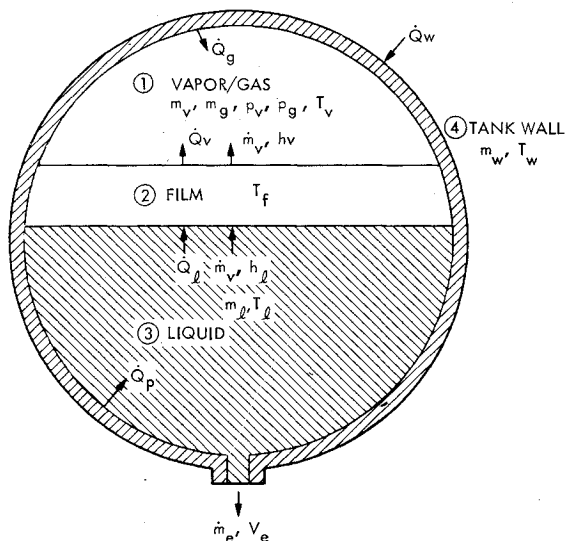


Fig. 2 Sketch of propellant supply tank showing control volumes.

the film layer, but is assumed the work done by the gas mixture is transmitted directly to the liquid. Throughout the blowdown process various heat transfers are also occurring. The proposed thermodynamic model accounts for all of the significant physical processes. Referring to Fig. 2, four control volumes are shown: one enveloping the mixture of pressurant gas and propellant vapor, another surrounding the liquid, the third is the film layer which is a control volume of infinitesimal thickness at the liquid and gas/vapor mixture interface, and the tank itself. The following assumptions are made to simplify the analysis: the propellant vapor and pressurant gas are ideal gases with constant specific heats, the gas/vapor mixture is a mixture of ideal gases, the pressurant gas is insoluble in the liquid, and the liquid has constant density and enthalpy of vaporization.

Referring to Fig. 2 the first law of thermodynamics for the gas/vapor control volume is

$$\dot{Q}_g + \dot{Q}_v - \dot{W} + \dot{m}_v h_v = \frac{d}{dt} (m_v u_v + m_g u_g) \quad (3a)$$

In Eq. (3a) \dot{Q}_g and \dot{Q}_v are the heat-transfer rates from the walls and film layer to the mixture, and \dot{W} the rate at which the gas/vapor mixture works on the liquid. The functional form of the heat- and work-transfer terms will be discussed shortly. By expanding the derivative, noting $h_v = u_v + R_v T_v$, $u_v = c_v T_v$, $u_g = c_g T_g$, and m_g is constant, Eq. (3a) can be simplified to

$$\dot{Q}_g + \dot{Q}_v - \dot{W} + \dot{m}_v R_v T_v = (m_v c_v + m_g c_g) \dot{T}_v \quad (3b)$$

Proceeding to region 2, the film layer, the first law can be written

$$\dot{Q}_l - \dot{Q}_v + \dot{m}_v h_l - \dot{m}_v h_v = 0 \quad (3c)$$

The film layer is considered infinitesimally thin, so that the energy storage term is negligible. The \dot{Q}_l term is the heat-transfer rate from the liquid to the film. The term $\dot{m}_v (h_v - h_l)$ can be rewritten as

$$\begin{aligned} \dot{m}_v [(h_v - h_{vs}) - (h_l - h_{ls}) + (h_{vs} - h_{ls})] \\ = \dot{m}_v [(c_v + R_v)(T_v - T_f) - c_l(T_l - T_f) + h_{fg}] \end{aligned}$$

where T_v and T_l are the gas/vapor mixture and liquid temperatures, respectively, T_f the film temperature (which is the saturation temperature corresponding to the partial pressure of vapor in the gas/vapor mixture) and h_{fg} the enthalpy of vaporization, which is assumed constant. We now consider the third control volume, the liquid region. The first law of thermodynamics becomes

$$\dot{Q}_p - \dot{Q}_l + \dot{W} - \dot{m}_v h_l - \dot{m}_l \left(h_l + \frac{V_l^2}{2} \right) = \frac{d}{dt} (m_l u_l) \quad (3d)$$

where \dot{Q}_p is the heat-transfer rate from the tank walls to the liquid. The kinetic energy of the evaporating mass is neglected, but the kinetic energy of the fluid being removed by the pump is included. By expanding the derivative, noting $d/dt (m_l) = -\dot{m}_e - \dot{m}_v$ from conservation of the liquid mass, $h_l \approx u_l$ (a good approximation for the range of conditions considered here), and $u_l = c_l T_l$, Eq. (3d) becomes

$$\dot{Q}_p - \dot{Q}_l + \dot{W} = \dot{m}_e (V_e^2/2) + m_l c_l \dot{T}_l \quad (3e)$$

The final control volume consists of the tank wall. Applying at the first law yields

$$\dot{Q}_w - \dot{Q}_p - \dot{Q}_g = \frac{d}{dt} (m_w u_w) \quad (3f)$$

where \dot{Q}_w is the heat-transfer rate from the surroundings to the tank exterior. Expanding the derivative, noting $u_w = c_w T_w$ and m_w is constant, yields

$$\dot{Q}_w - \dot{Q}_p - \dot{Q}_g = m_w c_w \dot{T}_w \quad (3g)$$

For spacecraft applications the acceleration experienced by the propellant can be very low relative to the Earth's gravitational acceleration. Studies^{15,16} on space storage of liquid propellants indicate that free convection will occur at g levels of 10^{-7} for small temperature changes. Thus heat-transfer terms appearing in Eqs. (3) are modeled as

$$\dot{Q}_g = h_g A_g (T_w - T_v) \quad (4a)$$

$$\dot{Q}_v = h_f A_f (T_f - T_v) \quad (4b)$$

$$\dot{Q}_l = h_s A_s (T_l - T_f) \quad (4c)$$

$$\dot{Q}_p = h_l A_s (T_w - T_l) \quad (4d)$$

$$\dot{Q}_w = h_w A_w (T_a - T_w) \quad (4e)$$

The values of the heat-transfer coefficients h_g , h_f , h_s , h_l and h_w can be estimated from free-convection heat-transfer correlations. Reference 6 gives an equation for the free-convection Nusselt number between a sphere and the fluid it encloses,

$$Nu_d = 0.098 (Gr_d Pr)^{0.345} \quad (5)$$

The equation is limited to the range of $Gr \cdot Pr$ product between 3×10^8 and 5×10^{11} . This equation is used to evaluate the heat-transfer coefficients between the tank wall and either the liquid propellant or the gas/vapor mixture.

For the heat transfer from the film layer to the gas/vapor mixture, a similar relationship developed for the upper surface of a heated plate was used.¹³

$$Nu = 0.14 (Gr_d Pr)^{0.333} \quad (6)$$

using the diameter of the liquid surface as the characteristic length.

Finally, for the heat-transfer coefficient between the liquid and the vapor film the average heat-transfer coefficient is estimated from the relationship developed for filmwise condensation on the horizontal tubes

$$h = 0.725 \left[\frac{\rho_l (\rho_l - \rho_v) g h_{fg} k_l^3}{\mu_d (T_v - T_l)} \right]^{1/4} \quad (7)$$

The parameter most subject to change in Eqs. (5-7) is the acceleration term g . For a specific application using a pumped propellant system (system parameters appear in Table 1), calculations with varying values of g showed that the heat-transfer coefficients remained essentially constant throughout the blowdown process. Changing the heat-transfer coefficients by a factor of three showed little or no effect on the results of the model. Hence the individual values of h are assumed to be constant. This may not be true in the more general case.

The heat-transfer areas referred to in Eq. (4) are indeed time varying. For a calculational convenience the area of the ullage/wall interface A_g (which does not include the film layer area) is correlated to the gas/vapor volume V_g and non-dimensionalized by the tank volume V_t for a spherical tank as

$$A_g / V_t^{2/3} = 4.0675 (V_g / V_t)^{0.62376} \quad (8a)$$

Given this correlation the film layer area A_f and liquid propellant/wall interface area A_l can be expressed as

$$\frac{A_f}{V_t^{2/3}} = \frac{A_g}{V_t^{2/3}} - 3.4211 \left(\frac{V_g}{V_t} \right)^{1.24752} \\ = 4.0675 \left(\frac{V_g}{V_t} \right)^{0.62376} - 3.411 \left(\frac{V_g}{V_t} \right)^{1.24752} \quad (8b)$$

$$\frac{A_f}{V_t^{2/3}} = \frac{A_w}{V_t^{2/3}} - \frac{A_g}{V_t^{2/3}} = \frac{\pi D^2}{V_t^{2/3}} - 4.0675 \left(\frac{V_g}{V_t} \right)^{0.62376} \quad (8c)$$

In Eqs. (8b) and (8c) A_w is the total surface area of the inside tank. The tank walls are sufficiently thin so that A_w is also approximately equal to the surface area of the outside of the tank. During the blowdown process the gas/vapor volume fraction V_g/V_t increases from roughly 0.05 to 0.95 and the error involved in using Eq. (8a) is typically 5% over this range of V_g/V_t . The maximum error of 9.2% occurs at $V_g/V_t = 0.5$.

The boundary work term appearing in Eqs. (3b) and (3e) is modeled as quasistatic work of expansion, $\dot{W} = p_t (dV_g/dt)$ where p_t is the time-varying total pressure of the gas/vapor mixture and V_g the volume occupied by the mixture at time t . Recognizing the total pressure p_t is the sum of partial pressures of gas and vapor, and both gases are ideal yields

$$p_t = p_v + p_g = p_v \left(1 + \frac{m_g R_g}{m_v R_v} \right) \quad (9a)$$

The term (dV_g/dt) can be evaluated from the ideal gas law for the vapor as

$$\dot{V}_g = \left[\frac{(\dot{m}_v T_v + m_v \dot{T}_v) p_v - m_v T_v \dot{p}_v}{p_v^2} \right] R_v \quad (9b)$$

and thus the boundary work term becomes

$$p_t \dot{V}_g = \left(1 + \frac{m_g R_g}{m_v R_v} \right) \left[\frac{(\dot{m}_v T_v + m_v \dot{T}_v) p_v - m_v T_v \dot{p}_v}{p_v} \right] R_v \quad (9c)$$

To complete the mathematical formulation of the problem, it is noted that the total volume is conserved

$$V_t = V_g + V_v = \frac{m_v R_v T_v}{p_v} + m_t v_t \quad (10a)$$

Table 1 Values of system parameters for pump-fed IPU test case

Parameter	Value
m_{t0}	2000 lbm (907 kg)
m_{v0}	0.582 lbm (0.264 kg)
m_g	0.0933 lbm (0.0423 kg)
m_w	30 lbm (13.6 kg)
R_v	0.0216 Btu/lbm · °R (90.4 J/kg · K)
R_g	0.496 Btu/lbm · °R (2075 J/kg · K)
c_v	0.180 Btu/lbm · °R (753 J/kg · K)
c_g	0.75 Btu/lbm · °R (3138 J/kg · K)
c_t	0.378 Btu/lbm · °R (1582 J/kg · K)
c_w	0.11 Btu/lbm · °R (460 J/kg · K)
h_{fg}	178 Btu/lbm (4.14 × 10 ⁵ J/kg)
v_t	0.01136 ft ³ /lbm (7.09 × 10 ⁻⁴ m ³ /kg)
T_0	530 °R (294 K)
p_{t0}	67 psia (0.462 MPa)
V_t	25.2 ft ³ (0.713 m ³)
\dot{m}_e	2.0 lbm/s (0.907 kg/s)
V_e	7.29 ft/s (2.22 m/s)
h_g	2.77 × 10 ⁻⁴ Btu/ft ² · h · °R (4.72 J/m ² · s · K)
h_s	6.94 × 10 ⁻⁴ Btu/ft ² · h · °R (14.1 J/m ² · s · K)
h_f	6.94 × 10 ⁻⁴ Btu/ft ² · h · °R (14.1 J/m ² · s · K)
h_t	4.17 × 10 ⁻³ Btu/ft ² · h · °R (84.7 J/m ² · s · K)
h_w	0.0 Btu/ft ² · h · °R (0.0 J/m ² · s · K)
a	3.02 × 10 ⁻³⁸ psia (8.828 × 10 ⁻³¹ Pa)
n	14.2

and the vapor pressure-saturation temperature relationship of the fluid can be approximated using thermodynamic data in a power law form

$$T_f = \left(\frac{p_v}{a} \right)^{1/n} \quad (10b)$$

where n and a are known constants.

The system of Eqs. (3-10) contains five independent differential equations for m_v , p_v , T_v , T_f , and T_w . From this set (which is not unique) all other state variables of interest p_t , p_g , T_f , V_g , etc., can be constructed. To facilitate the numerical solution the system of equations are non-dimensionalized by the variables listed in the Appendix. The resulting dimensionless system equations are

$$\frac{m_{t0}}{m_{v0}} \frac{V_t^{2/3}}{\dot{m}_e} \frac{h_g}{c_v} A_g^* (T_w^* - T_v^*) + \frac{m_{t0}}{m_{v0}} \frac{V_t^{2/3}}{\dot{m}_e} \frac{h_f}{c_v} A_f^* (T_f^* - T_v^*) \\ - \left(1 + \frac{m_g^* R_g}{m_v^* R_v} \right) \left[\frac{(m_v'^* T_v^* + T_v'^* m_v^*) p_v^* - p_v'^* m_v^* T_v^*}{p_v^*} \right] \frac{R_v}{c_v} \\ + m_v'^* \frac{R_v}{c_v} T_v^* = \left(m_v^* + m_g^* \frac{c_g}{c_v} \right) T_v'^* \quad (11a)$$

$$\frac{m_{t0}}{m_{v0}} \frac{V_t^{2/3}}{\dot{m}_e} \frac{h_s}{c_v} A_s^* (T_t^* - T_f^*) - \frac{m_{t0}}{m_{v0}} \frac{V_t^{2/3}}{\dot{m}_e} \frac{h_f}{c_v} A_f^* (T_f^* - T_v^*) \\ = m_v'^* \left[\left(1 + \frac{R_v}{c_v} \right) (T_v^* - T_f^*) - \frac{c_f}{c_v} (T_t^* - T_f^*) + \frac{h_{fg}}{c_v T_0} \right] \quad (11b)$$

$$\frac{V_t^{2/3}}{\dot{m}_e} \frac{h_t}{c_t} A_t^* (T_w^* - T_t^*) - \frac{V_t^{2/3}}{\dot{m}_e} \frac{h_s}{c_t} A_s^* (T_t^* - T_f^*) \\ + \left(1 + \frac{m_g^* R_g}{m_v^* R_v} \right) \left[\frac{(m_v'^* T_v^* + T_v'^* m_v^*) p_v^* - p_v'^* m_v^* T_v^*}{p_v^*} \right] \\ \times \frac{R_v}{c_t} \frac{m_{v0}}{m_{t0}} = T_t'^* m_t^* + \frac{V_e^2 \dot{m}_e}{2 c_t T_0} \quad (11c)$$

$$\frac{m_{t0}}{m_w} \frac{V_t^{2/3}}{\dot{m}_e c_w} A_w^* (T_a^* - T_w^*) - \frac{m_{t0}}{m_w} \frac{V_t^{2/3}}{\dot{m}_e c_w} A_t^* (T_w^* - T_t^*) \\ - \frac{m_{t0}}{m_w} \frac{V_t^{2/3}}{\dot{m}_e c_w} A_g^* (T_w^* - T_v^*) = T_w'^* \quad (11d)$$

$$T_f^* = \left(\frac{p_{t0} p_v^*}{c} \right)^{1/n} \frac{1}{T_0} \quad (11e)$$

In presenting the dimensionless system equations, the superscript ()' has been introduced denoting differentiation with respect to dimensionless time.

To cast Eqs. (11) into state space form similar to Eq. (2), straightforward but laborious algebra is required. The result is a set of ordinary, nonlinear differential equations suitable for integration as an initial value problem. In functional form Eq. (2) becomes

$$\dot{y} = f(y, t) - m_v'^* = f_1(m_v^*, p_v^*, T_v^*, T_w^*, T_t^*) \\ p_v'^* = f_2(m_v^*, p_v^*, T_v^*, T_w^*, T_t^*) \\ T_v'^* = f_3(m_v^*, p_v^*, T_v^*, T_w^*, T_t^*) \\ T_w'^* = f_4(m_v^*, p_v^*, T_v^*, T_w^*, T_t^*) \\ T_t'^* = f_5(m_v^*, p_v^*, T_v^*, T_w^*, T_t^*) \quad (12)$$

where at $t^* = 0$, $m_v^* = p_v^* = T_v^* = T_w^* = T_t^* = 1$. Equation (12) implies that the input (forcing) functions $u_1(t) \dots u_r(t)$ are all zero, which is appropriate for this particular problem.

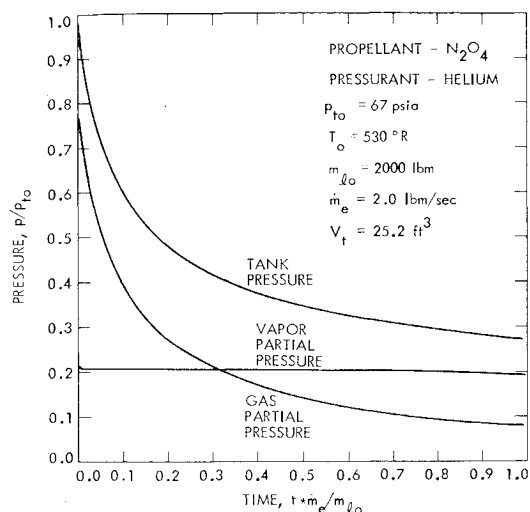


Fig. 3 Dimensionless pressure p_t^* , p_v^* , p_g^* vs dimensionless time t^* .

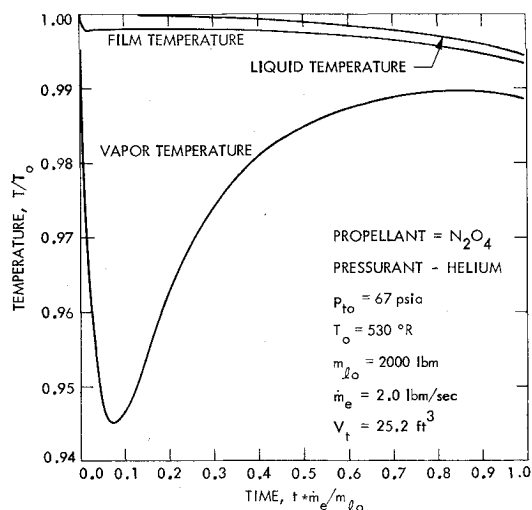


Fig. 4 Dimensionless temperature T_v^* , T_l^* , T_f^* vs dimensionless t^* .

Results and Discussion

The results of numerically integrating the system differential equations, Eq. (12), for a specific application are shown in Figs. 3-6. The case taken was for that of 2000 lbm (907 kg) of N_2O_4 in a spherical tank. This amount of oxidizer is approximately one-half that required to insert an 8820 lbm (4000 kg) spacecraft (launch mass) into orbit about Venus. The spacecraft design includes four tanks, two oxidizer and two fuel. The system parameters are listed in detail in Table 1.

The N_2O_4 propellant has a high vapor pressure, roughly 14.7 psia (0.101 MPa) at 70°F (21°C) and thus it is sensitive to delivering the proper net positive suction head to the pump.

The particular numerical scheme used was an initial value ODE routine using the Adams-Moulton predictor-corrector multistep technique. The routine can adjust the order of the method to suit the user specified accuracy while maximizing the time step. The minimum order is two and third- or fourth-order accuracy is obtainable. A 0.1% error tolerance was used throughout the integration.

Implemented on a Univac 1100/81 system, the computer program uses about 39K words of main memory and the entire integration from the initial conditions to tank depletion takes about 10 CPU seconds.

Of primary importance in this study are the total tank pressure, propellant vapor partial pressure, and pressurant gas partial pressure. All are shown in Fig. 3. From the tank

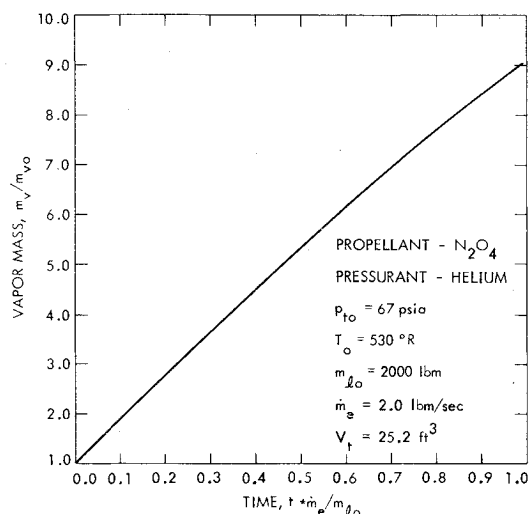


Fig. 5 Dimensionless propellant vapor mass m_v^* vs dimensionless time t^* .

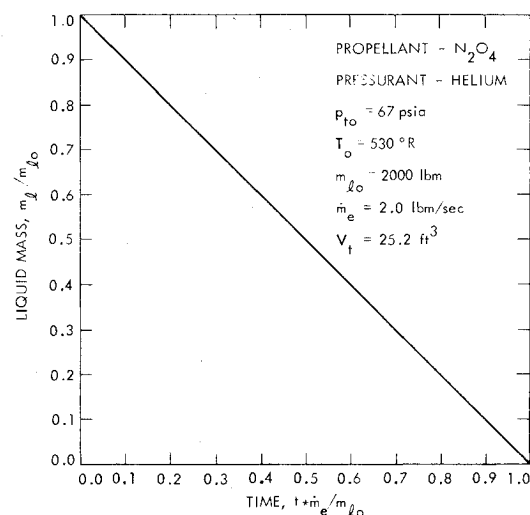


Fig. 6 Dimensionless propellant liquid mass m_l^* vs dimensionless time t^* .

pressure and propellant vapor partial pressure it can be determined if the required value of NPSH exists throughout the orbital insertion. Figure 3 shows the total tank pressure is continuously decreasing while the vapor partial pressure remains virtually constant. Calculating the NPSH as $t^* \rightarrow 1$ yields, from Eq. (1)

$$\text{NPSH} = \frac{(p_t^* - p_v^*)}{\rho} p_{t0} = 8.8 \text{ ft of propellant}$$

which is sufficient for the pump currently included in the system design.

In this calculation the gravity head ρgh due to the spacecraft acceleration was neglected, as the physical location of the pump, i.e., the value of h , with respect to the storage tanks is currently unknown. It is assumed that the pumps will be mounted aft of the storage tanks, hence the head provided will be actually greater (perhaps as much as 4 ft of propellant) than that merely due to the pressure head.

Figure 4 shows the dimensionless liquid temperature, film temperature, and vapor temperature as a function of dimensionless time. It is seen that the liquid and film temperatures remain virtually constant changing less than 1%. The vapor temperature exhibits a sharp drop to $T_v^* = 0.945$ at $t^* = 0.074$ and a gradual increase as $t^* \rightarrow 1$. Physically the expansion of the gas is essentially adiabatic until the tem-

perature differences between the gas and liquid are large enough and the tank pressure drops sufficiently, allowing transfer of mass and energy into the ullage volume from the liquid. In this way the tank is forced toward equilibrium.

The vapor propellant mass and liquid propellant mass are depicted in Figs. 5 and 6. The vapor mass continuously increases, corresponding to the propellant vaporization. However, the absolute amount of propellant mass in the vapor phase is negligible compared with the liquid propellant mass over most of the blowdown process. The result is that m_t^* exhibits a linearly decreasing behavior corresponding to constant mass removal by the pump.

Although this application is specific to a particular implementation of a pump-fed, low-pressure storage tank, the method and system of Eq. (12) can be used to analyze different fluids with different initial conditions. Further, with minor modifications to Eq. (12) one can calculate the results for various tank shapes and systems, such as cylindrical tanks and pressure-fed systems where the mass flow out of the tank is not constant.

Conclusions

The state space form of the equations of motion for a propellant supply system was developed into a compact and convenient modeling form suitable for numerical simulation. Further, this form of a system of ODEs lends itself to quick and efficient computer coding to perform the calculations. This modeling formalism is also applicable to any tank blowdown process where a liquid is expelled by a gas pressurant.

The results of the application of the model to an N_2O_4 supply system operated in a blowdown mode indicate the viability of a pump-fed IPU on planetary spacecraft. The model demonstrates that a pump-fed IPU is capable of supplying required propellant flow rates with sufficient NPSH during typical orbital insertion maneuvers.

The largest uncertainty associated with the pump-fed IPU is the cost required to develop it. In essence there is a tradeoff between the cost associated with the pump and drive system development and those costs of a pressurization system including pressurant tank, regulator, and necessary control/delivery system. Related studies have indicated that the costs of two different approaches are gradually becoming comparable.

Appendix

Included here is a compilation of the dimensionless variables used in the nondimensionalizing of the state equations [Eqs. (11)].

$$A_g^* = A_g / V_t^{2/3}$$

$$T_a^* = T_a / T_0$$

$$A_f^* = A_f / V_t^{2/3}$$

$$T_f^* = T_f / T_0$$

$$A_t^* = A_t / V_t^{2/3}$$

$$T_t^* = T_t / T_0$$

$$A_w^* = A_w / V_t^{2/3}$$

$$T_v^* = T_v / T_0$$

$$m_t^* = m_t / m_{t0}$$

$$T_w^* = T_w / T_0$$

$$m_v^* = m_v / m_{v0}$$

$$t^* = tm_e / m_{t0}$$

$$p_t^* = p_t / p_{t0}$$

$$V_g^* = V_g / V_t$$

$$p_v^* = p_v / p_{t0}$$

References

- ¹Estey, P.N., "A Pump-Fed Bipropellant Propulsion System for Planetary Missions," Paper presented at 1980 JANNAP Propulsion Meeting, Monterey, Calif., March 1980.
- ²Estey, P.N. and Boretz, J.E., "A Pump-Fed Propulsion System for Earth-Orbiting Satellites," Paper presented at 1981 JANNAP Propulsion Meeting, New Orleans, May 1981.
- ³Auslander, T.W., Boretz, J.E., and Estey, P.N., "Selection of a Pump-Fed Propulsion System for Planetary Exploration Missions," Paper 81, July 1981.
- ⁴Nein, M.E. and Thompson, J.F., "Prediction of Propellant Tank Pressurization Requirements by Dimensional Analysis," NASA TN D-3451, June 1966.
- ⁵Epstein, M., Georgius, H.K., Anderson, R.E., "A Generalized Propellant Tank Pressurization Analysis," *International Advances in Cryogenic Engineering*, Vol. 10, Aug. 1964.
- ⁶Roudebush, W.H., "An Analysis of the Problem of Tank Pressurization During Outflow," NASA TN D-2585, Jan. 1965.
- ⁷Arnett, R.W. and Voth, R.O., "A Computer Program for the Calculation of Thermal Stratification and Self-Pressurization in a Liquid Hydrogen Tank," NASA CR-2026, May 1972.
- ⁸Brintzenhoff, A.L., "PSOP-D Users Manual," Jet Propulsion Laboratory, Rept. IOM 915-31/417, Feb. 1972.
- ⁹Page, R., "Analysis of Propellant Tank Pressurization Computer Program Users Manual," Martin Marietta Aerospace Corporation, 1968.
- ¹⁰Pasley, G.F., "Optimization of Stored Pressurant Supply for Liquid Propulsion Systems," *Journal of Spacecraft and Rockets*, Vol. 7, Dec. 1970, pp. 1478-1480.
- ¹¹Pasley, G.F., "Prediction of Tank Pressure History in a Blowdown Propellant Feed System," *Journal of Spacecraft and Rockets*, Vol. 9, June 1972, pp. 473-475.
- ¹²Hearn, H.C., "Feasibility of Simple Bipropellant Blowdown Systems," *Journal of Spacecraft and Rockets*, Vol. 17, March-April 1980, pp. 157-158.
- ¹³Holman, J.P., *Heat Transfer*, McGraw Hill Book Co., New York, 1972.
- ¹⁴Ring, E., *Rocket Propellant and Pressurization Systems*, Prentice Hall, Englewood Cliffs, N.J., 1964.
- ¹⁵Holmes, L.A. and Schwartz, S.A., "The Thermodynamics of Space Storage of Liquid Propellants," Douglas Aircraft, Inc., 1965.
- ¹⁶Reynolds, W.C. and Satterlee, H.M., "Liquid Propellant Behavior at Low and Zero g," *The Dynamic Behavior of Liquids in Moving Containers*, NASA-SP-106, 1966.